

RESEARCH PAPER

Finite Element Analysis of Wire Deflection and Temperature Effects on Ceramic Orthodontic Bracket Slot Deformation

Sarah Mahmood Khudhur, Muhammad Fauzinizam bin Razali *, Abdus Samad bin Mahmud

School of Mechanical Engineering, Engineering Campus, Universiti Sains Malaysia, Pulau Pinang, Malaysia

ARTICLE INFO

Article History:

Received 12 January 2025

Accepted 18 March 2025

Published 01 April 2025

Keywords:

Ceramic bracket

Deflection

Finite Element Analysis

Modified 3-point bending test

Temperature

ABSTRACT

Orthodontic brackets especially those made from alumina-based ceramics have become more popular due to their superior aesthetics and biocompatibility. However, their brittleness remains a drawback, as they are more likely to chip or break during treatment compared to metal brackets. The objective of this study is to analyze the mechanical deformation of ceramic brackets under varying archwire deflection and oral temperature using finite element analysis. Aesthetic Roth prescription of polycrystalline ceramic bracket with “0.022” inches slot and rectangular NiTi archwire were used. A three-dimensional finite element model was developed to simulate a modified 3-point bending test at magnitudes of deflection ranges from 1 to 6 mm. Temperature ranges used was from 26 °C to 56 °C which represented a range of typical oral temperature variations. Stress and strain were recorded at specific reference points within bracket slot at both loading and unloading cycle. The simulation results reveal that deformation in ceramic bracket slots was consistently concentrated at the corner regions across all three ceramic brackets. Both increasing wire deflection and temperature significantly elevated stress levels, often surpassing the fracture strength of the brackets, particularly during the loading cycle. The maximum stress observed during loading was 411.02 MPa at 56 °C for a 6 mm deflection case. Although the unloading cycle exhibited lower stress levels, deflections exceeding 2 mm still posed failure risks, with a maximum recorded stress of 220.19 MPa at 56 °C for a 6 mm deflection case. These findings highlight the critical influence of wire deflection and temperature on the mechanical deformation of ceramic brackets. These findings underscore the critical role of archwire deflection and oral temperature in managing stress distribution and preventing fracture in ceramic brackets. Clinicians should carefully evaluate bracket materials, particularly in cases involving substantial wire activation or elevated oral temperatures and advise patients on temperature-sensitive dietary habits to mitigate the risk of premature bracket failure.

How to cite this article

Khudhur S., Razali M., Mahmud A. Finite Element Analysis of Wire Deflection and Temperature Effects on Ceramic Orthodontic Bracket Slot Deformation J Nanostruct, 2025; 15(2):487-498. DOI: 10.22052/JNS.2025.02.009

INTRODUCTION

During orthodontic treatment, the tooth moves in different orientations and direction at three major stages, leveling and alignment, space closure and correction of molar relationship, and

* Corresponding Author Email: mefauzinizam@usm.my

finishing treatment. The desire tooth movement achieved by using fixed appliances which consists of bracket, archwire and ligatures. In a famous malocclusion case of highly displaced canine tooth, the installation of the appliance is started



This work is licensed under the Creative Commons Attribution 4.0 International License.

To view a copy of this license, visit <http://creativecommons.org/licenses/by/4.0/>.

by bonding the dental brackets, an archwire is then carefully inserted into the bracket slots, following the irregularity of the bracket position, which causes localized bending across the wire length. To secure the archwire in place, small rubber rings, fine wires, or a metal clip—depending on the type of bracket used—are employed. Over time, as the archwire gradually returns to its original straight shape, it exerts a light force on the misaligned tooth, guiding it downward in the direction of the bending recovery [1-4]. It was reported in many studies that the treatment time is ranging from 14 to 33 months with no assessing to treatment outcomes quality [5-7]. A tooth movement rate of approximately 1.0 mm per month is considered optimal and can be achieved by applying forces ranging from 0.10 N to 1.20 N [8]. This force range is effective in promoting efficient tooth movement while ensuring maximum comfort for the patient.

A wide range of archwire alloys are available to generate the biomechanical forces like stainless-steel, beta-titanium and nickel-titanium alloy. Superelastic NiTi wires are widely used for leveling and aligning teeth, whereas beta titanium and stainless steel wires are typically preferred for space closure and detailing. A variety of round and rectangular archwires in different sizes are available on the market. Despite the wide range of sizes, materials, and shapes, the choice of archwire ultimately depends on the treatment stage and objectives rather than patient preferences [3]. Round archwires are typically used during the initial stages of orthodontic treatment to align and level irregular teeth. As tooth alignment improves over the course of treatment, the orthodontist advances to use a rectangular archwires [9,10]. The extent of archwire bending varies throughout treatment and is influenced by the clinical requirements at each stage. Early in treatment, archwires are bent more significantly to accommodate irregularities, whereas later stages involve less bending as the teeth approach the final alignment. It is well established that for small deflections, NiTi archwires exhibit a superelastic plateau on the force-deflection curve, maintaining a nearly constant and low force over a range of deflections during bending and recovery [11]. This force behavior allows for continuous, gentle force application, ideal for tooth movement.

Ceramic orthodontic brackets are made of aluminum oxide (Al_2O_3) which called alumina. Although aesthetic is an inherent advantage

of these brackets, they do have several disadvantages including high brittleness and high fracture risk [12,13]. One of the common causes of ceramic bracket breakage is the application of excessive force during archwire engagement or adjustments. Anisa et al. conducted a fracture strength test on polycrystalline ceramic brackets by applying a vertical force perpendicular to the bracket's long axis, specifically on the disto-incisal wings, until failure occurred. The study reported a maximum fracture strength of 59.25 MPa [14]. While Nick Beumsu conducted a fracture strength test by applying a vertical force on the mesial incisal wing of each polycrystalline bracket, recording the force at the point of tie wing fracture as the fracture strength. The study found that the fracture strength of polycrystalline brackets ranged between 84.99 MPa and 301.03 MPa. [15]. Another study by Johnson et al., who tested the tensile fracture strength of ceramic brackets by applying a tensile load directly under the disto-incisal tie wing until failure, reported that the fracture strength of polycrystalline true-twin ceramic orthodontic bracket is 117.76 MPa [16].

Finite element analysis (FEA) studies have primarily examined bracket deformation under tipping and torque forces, two key mechanical conditions in orthodontics. Tipping forces applied in these studies ranged from 0.004 N to 1.225 N [17,18], while torque forces varied from 0.028 N to 28.3 N [17,19]. The stress distribution observed during these tests showed significant variation, with ceramic brackets experiencing stresses ranging from 0.008 MPa to 125.5 MPa under tipping and between 43.6 MPa and 468.1 MPa under torque forces [17-19]. These findings provide valuable insights into bracket performance during tipping and torque application. However, despite the detailed investigations into tipping and torque, limited research has focused on bracket deformation during the leveling stage. This leaves a gap in understanding how brackets behave during leveling and limits the knowledge on the deformation of brackets under these conditions.

Although oral temperature influences the NiTi wire properties, which indirectly influences the deformation scale of the bracket slot, studies on its effect, particularly on ceramic bracket slot paired with NiTi archwire remain limited and underexplored to the best of our knowledge. Therefore, this study aimed to investigate the mechanical deformation of the ceramic bracket

slot when paired with a NiTi archwire under varying temperatures and wire deflections. A finite element analysis method was utilized to simulate temperature variations and wire deflection ranges under clinically relevant conditions. This method allows for an accurate and controlled assessment of stress and strain distributions within the ceramic bracket slot, providing insight into its mechanical response. The contribution of this work lies in offering a deeper understanding of how temperature and deflection variations impact ceramic brackets' mechanical performance, helping orthodontists in selecting appropriate brackets and treatment protocols to minimize bracket failure risk.

MATERIALS AND METHOD

Experimental testing

In this study, two experimental analyses were performed: uniaxial tensile testing and a modified three-point bending test. The uniaxial tensile test was conducted to determine the mechanical properties of the NiTi wire, specifically to define its superelastic behavior for incorporation into the material subroutine. The modified three-point bending test was carried out, involving the engagement of three brackets during the test. The results of the bending test were utilized to validate the force-deflection curve obtained from the numerical model.

The uniaxial test conducted on an Instron universal testing machine (model 3367) equipped with a 30-kN load cell. The specimens were cut from the straight-end portions of the arch-shaped wires. The testing procedures followed the ISO 15841 standard for orthodontic wires. Each specimen measured 50 mm in length, with a 20 mm gauge length and 15 mm at each end for gripping. During testing, the specimens were stretched to a displacement of 2.5 mm (12.5% strain) and then unloaded to zero displacement at a rate of 1.0 mm/min. The tests were performed at three temperatures 26°C, 36°C, and 46°C., when necessary, a heater with an accuracy of $\pm 1^\circ\text{C}$ was used to maintain the desired environmental temperature, as shown in Fig. 1a. The uniaxial test was conducted three times to ensure result consistency, with a new specimen used for each trial. Subsequently, the superelastic material properties were selected based on a single stress-strain curve obtained at 26°C.

The force-deflection behavior exerted by the

superelastic archwires in bracket configurations was evaluated using a modified three-point bending. As shown in Fig. 1b, rather than bending the archwire over three points, this setup utilized three aligned brackets with 0.56 mm slot height and 3 mm slot width. The central bracket and the adjacent ones were mounted on the movable indenter and fixed supports, respectively. These three polycrystalline ceramic brackets represented a lateral incisor, a canine, and a first premolar, corresponding to a portion of an upper-left maxillary arch. The bending test was conducted using the same universal testing machine, fitted with a customized compressive loading jig. A lower load cell with a 500 N capacity was used to enhance the load measurement sensitivity. The clinical scale of the apparatus was set by positioning the brackets 7.5 mm apart, based on the average distance between the midpoints of the canine, incisor, and premolar on a maxillary arch [1]. The brackets were securely glued to the movable indenter and the mounting base. The wire was deflected by 4.0 mm at the same crosshead speed of 1.0 mm/min, with the load applied along the wire's thickness. The force was then unloaded to allow the wire to return to its original position at the same speed. The entire test setup was conducted at 26°C, using a heater.

Shape memory alloy model

A built-in user material subroutine (UMAT/ Nitinol) in Abaqus 6.13.1 was employed to simulate the superelasticity of NiTi wire. Auricchio and Taylor established this subroutine based on a generalized plasticity theory that decomposes strain components into purely elastic and transformational strains [1]. Because its good agreement with experimental result involving bending type deformation, this model was chosen over other viable macro scales constitutive models [1]. Table 1 illustrate the mechanical properties of NiTi archwire obtained from uniaxial test at 26 °C.

Finite element simulation of a bending test

A finite element model of the modified 3-point bending test was developed with two main components, the NiTi archwire and the ceramic bracket. The 30 mm length wire specimen was modeled by using linear hexahedral elements with reduced integration (C3D8R). The benefit of using these reduced-integration elements is that they utilize a lower-order integration method to

calculate the element matrices, compared to the full-order integration elements (C3D8). The NiTi archwire used in this study had a cross-sectional dimension of 0.40 mm in height and 0.56 mm in width, with a total length of 30 mm. The ceramic bracket featured a width of 3 mm and a slot height of 0.56 mm, ensuring compatibility with the archwire dimensions. A total of 23,760 and 17,280 elements were chosen for the archwire and ceramic bracket respectively, as it resulted to shorter computational period. The determination

of elements number was based on the mesh independence study.

The brackets also modelled using 8-node linear brick elements with reduced integration (C3D8R). The dimensions of the bracket slot were obtained by directly measuring from scanning electron microscope images. Both the wire and bracket components were partitioned into several sections to facilitate the contact pairing process during assembly. Ceramic brackets type used (Acclaim Roth) has an angulation around 9° for

Table 1. Material data for superelastic NiTi wire model (T= 26 °C).

Parameter	Description	Value (unit)
EA	Austenite elasticity	45 (GPa)
(ν_A)	Austenite Poisson's ratio	0.33
EM	Martensite elasticity	16 (GPa)
(ν_M)	Martensite Poisson's ratio	0.33
(ϵ_L)	Transformation strain	0.085
($\delta\sigma/\delta T$) _L	Stress-temperature rate during loading	6.7(MPa/°C)
σ_{SL}	Critical stress for start of forward transformation	380 (MPa)
σ_{EL}	Critical stress for end of forward transformation	410 (MPa)
T ₀	Reference temperature	26 °C
($\delta\sigma/\delta T$) _U	Stress-temperature rate during unloading	6.7(MPa/°C)
σ_{SU}	Critical stress for start of reverse transformation	200 (MPa)
σ_{EU}	Critical stress for end of reverse transformation	120 (MPa)
σ_{SCL}	Critical stress for start of compression transformation	456 (MPa)
(ϵ_V)	Volumetric transformation strain	0.085

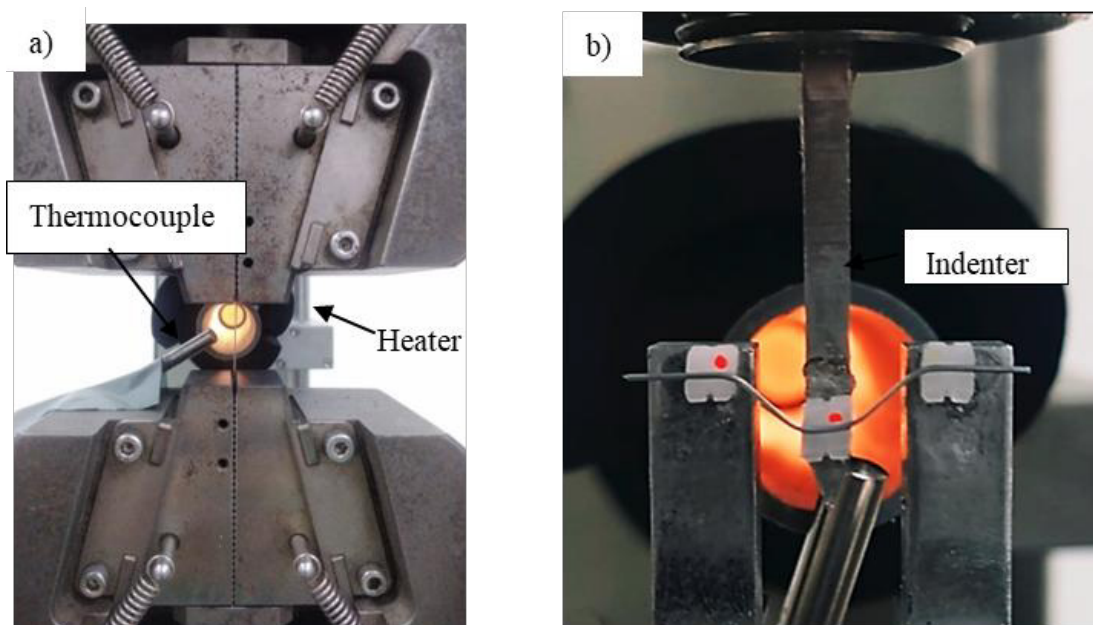


Fig. 1. a) Uniaxial tensile test setup, b) Three-bracket bending setup.

lateral, 11° for cuspid and 0° for first bicuspid [20]. These values designed to achieve specific tooth movement during orthodontic treatment. The Young's modulus and Poisson's ratio for ceramic bracket was 380000 MPa and 0.29 respectively, as reported in literature [21].

As shown in Fig. 2, the bracket and wire components were assembled to define the analysis model. Three brackets were included in the analysis, each associated with a distinct reference point (RP). This method ensures that any motion or constraints applied to a reference

point are transferred to the entire bracket. The reference points were designated as RP-1, RP-2, and RP-3, corresponding to the middle, left, and right bracket positions, respectively. These reference points located on the back surfaces of the brackets. Only the central bracket was set to move in y-direction in a displacement rate of 1mm/min, while the adjacent brackets constrained to be fixed in all directions ($U_x = U_y = U_z = 0$). The coefficient of friction was set to 0.4. It was reported in literature that the coefficient of friction between NiTi archwire and ceramic bracket

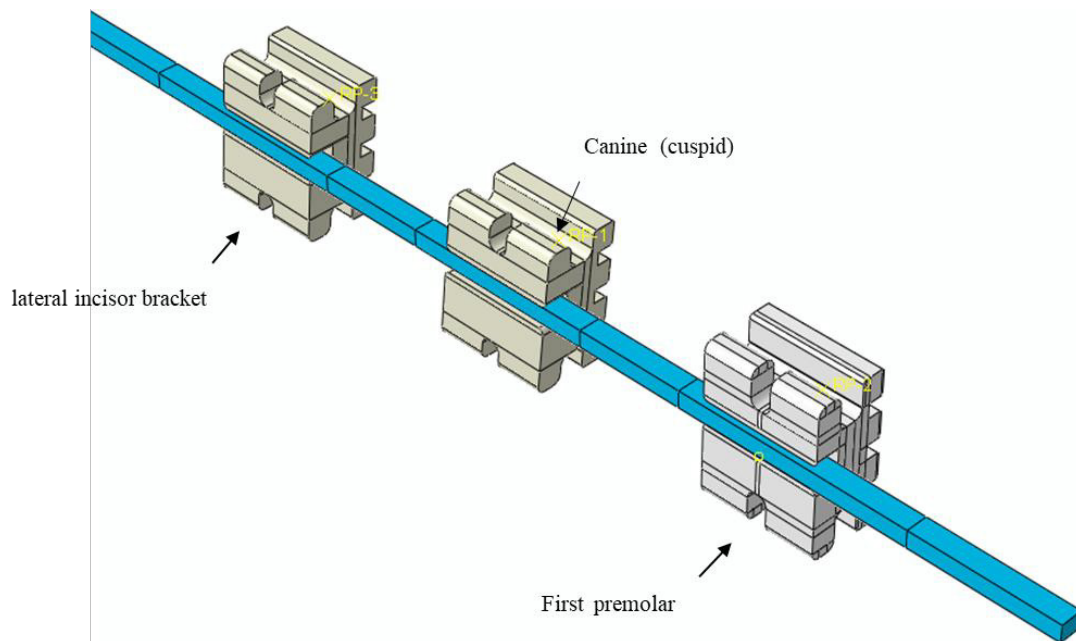


Fig. 2. NiTi wire and ceramic bracket assembly.

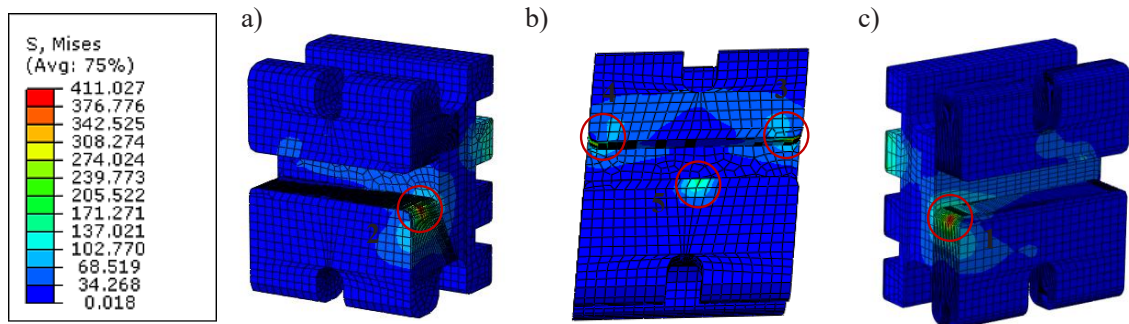


Fig. 3. Illustration of different spots experienced changeable stress level during loading and unloading for a) lateral incisor bracket, b) canine (cuspid) bracket, and c) first premolar bracket.

surface to be in the range of 0.4 – 0.5 [3]. The wire set to be deflected to 1, 2, 3, 4, 5, and 6 mm at four different temperatures of 26 °C, 36 °C, 46 °C, 56 °C respectively. The four temperatures used in the present study represents the oral temperature for different cases; behavior at the time of installation (26 °C), behavior inside the oral environment (36 °C), behavior during exposure to warm food intake (46 °C) and behavior during consuming hot drinks like coffee (56 °C) [1,22]. The selected deflection ranges were determined based on typical clinical conditions observed during orthodontic treatment [1].

The color contour in Fig. 3 illustrates the degree

of deformation of the bracket at 6 mm wire deflection during the loading and unloading cycle at 56 °C. The red contour spot indicates regions experiencing high stress due to the applied bending load on the archwire, while the blue contour spot represents areas with minimal deformation. Five critical spots were identified across the three brackets for mechanical deformation assessment, as indicated by the red circles. These spots were chosen as they experienced considerable von Mises stress changes due to the sliding of the archwire within the bracket slot during loading and unloading cycle. Point 1 represents node number 15238 in first premolar bracket, and point

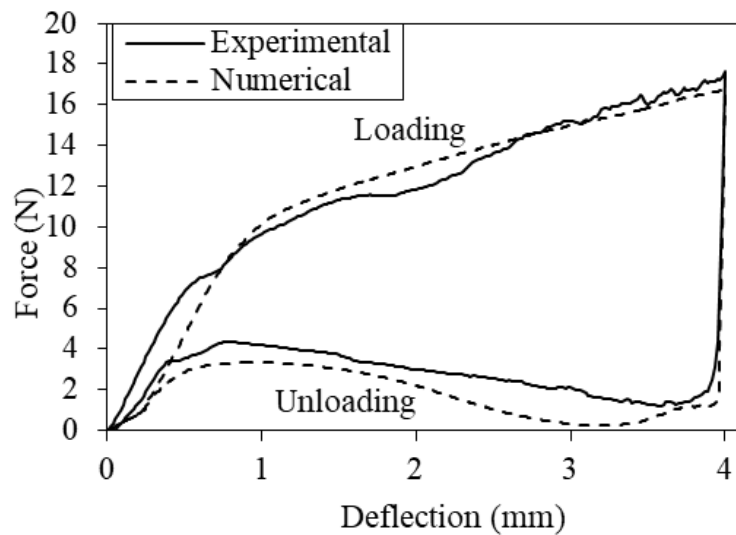


Fig. 4. Force-deflection curve of NiTi wire in a modified three-point bending test.

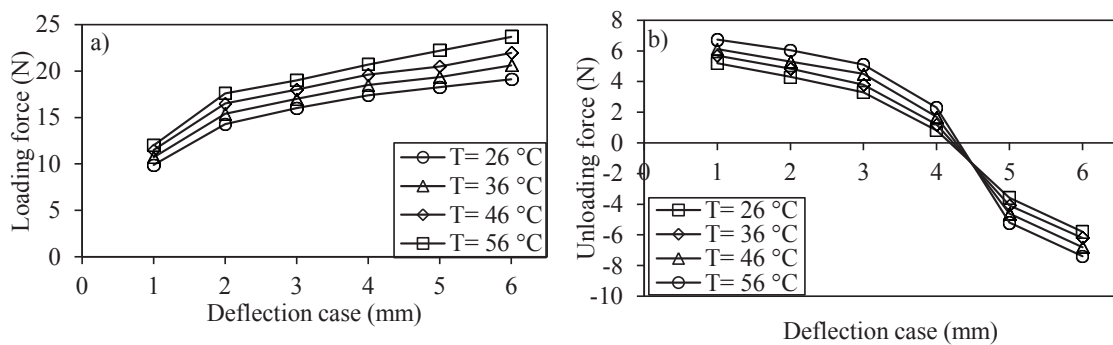


Fig. 5. Illustration of maximum force during a) loading, and b) after 0.5mm deflection recovery.

2 represents node number 6856 in lateral incisor bracket, while points 3, 4, and 5 represents nodes number 5535, 805, and 1171, respectively in canine bracket.

RESULTS AND DISCUSSION

Fig. 4 presents a comparison of the force-deflection plots for NiTi archwire obtained from both experimental and simulation results under 4 mm bending at 26 °C. The experimental data, represented by the solid line, and the numerical results, represented by the dashed line, show a similar trend throughout the deflection range. The loading cycle began with a small linear slope up to 0.25 mm of deflection, representing the bending stiffness of the wire before making a contact with the top lateral edges of the bracket. Once the contact was established, the wire became more constrained within the bracket slot, thus yielded a steeper slope before reaching the plateau at about 1 mm of deflection.

The unloading cycle starts with a sudden force drop which is a result of the stress-induced martensitic transformation in the NiTi archwire. When the applied force exceeds a critical stress level, the material undergoes a phase transformation from the austenite phase to the martensite phase. The force drop represents the onset of this transformation. This agreement between the two curves validates the accuracy of the numerical model in predicting the mechanical response of the NiTi archwire under the simulated conditions.

Fig. 5a presents the loading force exerted by the NiTi archwires when bent at different temperatures and deflection cases in the modified bending setup. The force magnitudes for each deflection case represent the maximum force recorded during the loading cycle from the force-deflection curve. In overall, this plot illustrates the influence of temperature variations on the mechanical response of the NiTi wire in a ceramic bracket system. At a given temperature, it is seen that the force exerted by the NiTi wire increases as the wire being deflected at a higher magnitude. At 56 °C, the force magnitude increased from 12 N in the case of 1 mm to 23.69 N in the case of 6 mm. Additionally, the force values at higher temperatures consistently exceed those at lower temperatures, with the variation becoming more pronounced at larger deflections. This trend highlights the temperature-sensitive superelastic

behavior of the NiTi wire. In the case of 6 mm deflection, the force magnitude increased from 19.13 N at 26 °C to 23.69 N at 56 °C.

Fig. 5b presents the unloading force exerted by the NiTi archwires when bent at different temperatures and deflection case in the modified bending setup. The unloading force reported in Fig. 5b was measured after the wire was unloaded by 0.5 mm from its maximum deflection. This measurement captures the magnitude of force released by the NiTi archwire as it transitions from the austenite phase to the martensite phase upon the release of the bending load. In overall, the unloading force exerted by the NiTi wire increases as the deflection decreases. As the deflection magnitude increases, the unloading force decreases, initially remaining positive at lower deflections before transitioning to negative at higher deflections. For instance, at 36 °C, the unloading force starts at 5.69 N in the case of 1 mm deflection and decreases to 1.2 N at 4 mm deflection case, before turning negative, reaching -6.2 N at 6 mm deflection case. The transition from positive to negative unloading force occurs between 4 mm and 5 mm deflection cases. Additionally, for a given deflection case, the unloading force generally increases as the temperature increases. At 4 mm deflection case, the unloading force at 26 °C is 0.82 N and progressively increase with increasing temperature, reaching 1.2 N at 36 °C, 1.7 N at 46 °C, and 2.3 N at 56 °C.

The stress and strain values measured at critical points on the bracket model under different deflections and temperatures are presented in Table 2. As the deflection and temperature increase, the stress and strain values exhibit a consistent pattern of change. For instance, the stress at the bracket corners gradually increased with increasing wire deflection. During loading at 26 °C, the stress range increased from 0.67–124.78 MPa in the 1 mm case to 91.96–218.84 MPa in the 6 mm case. Similarly, the corresponding strain values increased from 5.4×10^{-7} – 1.3×10^{-4} to 8.9×10^{-5} – 2.4×10^{-4} mm/mm for the same temperature and deflection range. Additionally, the stress at the bracket corners continues to increase with increasing temperature. In the case of 6 mm, the stress range escalates from 91.96–218.84 MPa at 26 °C to 104.0–269.46 MPa at 56 °C, while the strain also rises slightly.

Table 3 presents stress and strain measured at five critical points on the bracket model after the

NiTi archwires recovered by 0.5 mm of deflection. As the wire deflection decrease, the stress in the ceramic bracket also decreases. For instance, at 26 °C the stress range decreased from 88.72 – 94.41 MPa in the case of 6 mm deflection to 0.09 – 27.38 MPa in the case of 1 mm deflection, while the corresponding strain range decreased from $7.7 \times 10^{-5} - 9 \times 10^{-5}$ mm/mm to $8.1 \times 10^{-8} - 1.9 \times 10^{-5}$ mm/mm for same temperature and deflection case. With increasing temperature, the bracket stress generally increases. In the case of 6 mm deflection, the stress range increased from 88.72 – 94.41 MPa at 26 °C to 116.55 – 124.91 MPa at 56 °C, with obvious increase in strain range as well. Interestingly, for a given bending setting, the bracket stress observed during the unloading cycle was consistently lower than that recorded in Table 2 during the loading cycle.

Table 4 highlights the maximum stress and strain values observed in the ceramic bracket slot during loading and unloading. These values

were exhibited by nodes number 15241 (Spot 1) in first premolar bracket and 6854 (Spot 2) in lateral incisor bracket model during loading and unloading, respectively. For the loading cycle, as the magnitude of applied deflection increases, both stress and strain values rise significantly at all temperatures. For instance, at 26°C, the stress increases from 172.9 MPa in the 1 mm case to 327.8 MPa in the 6 mm case, while the strain rises from 2.7×10^{-4} to 4.8×10^{-4} mm/mm. This trend is consistent across higher temperatures, where the stresses and strains are noticeably larger. In the case of 6 mm, stress escalates from 327.8 MPa to 411.02 MPa when temperature increase from 26 °C to 56 °C, with corresponding strain increasing from 4.8×10^{-4} to 6.2×10^{-4} mm/mm. While for the unloading cycle, as the applied deflection decreases, the magnitude of bracket stress also decreases. For instance, at 26 °C the stress decreases from 200.35 MPa in the 6 mm case to 41.80 MPa in the case of 1 mm, while strain also

Table 2. Stress and strain in ceramic bracket at different deflections and temperatures during loading.

Deflection case (mm)	Point n o.	26 °C		36 °C		46 °C		56 °C	
		Stress (MPa)	Strain (mm/mm)						
1	1	124.78	1.3×10^{-4}	138.49	1.4×10^{-4}	145.24	1.5×10^{-4}	150.02	1.6×10^{-4}
	2	115.30	1.2×10^{-4}	127.26	1.3×10^{-4}	133.30	1.4×10^{-4}	137.61	1.4×10^{-4}
	3	55.16	6.9×10^{-5}	59.12	7.3×10^{-5}	61.88	7.6×10^{-5}	63.36	7.7×10^{-5}
	4	67.62	5.4×10^{-5}	73.40	5.7×10^{-5}	76.58	6.0×10^{-5}	78.05	6.1×10^{-5}
	5	0.67	5.4×10^{-7}	0.74	5.9×10^{-7}	0.78	6.3×10^{-7}	0.81	6.5×10^{-7}
2	1	157.69	1.4×10^{-4}	178.45	1.6×10^{-4}	202.09	1.8×10^{-4}	226.70	2.1×10^{-4}
	2	151.31	1.5×10^{-4}	169.56	1.7×10^{-4}	192.35	1.9×10^{-4}	213.06	2.2×10^{-4}
	3	71.18	7.4×10^{-5}	76.87	7.6×10^{-5}	82.63	7.7×10^{-5}	91.43	7.9×10^{-5}
	4	99.37	7.2×10^{-5}	109.04	8.3×10^{-5}	118.74	8.8×10^{-5}	131.36	9.7×10^{-5}
	5	12.20	1.3×10^{-5}	13.57	7.9×10^{-6}	14.39	3.6×10^{-6}	15.07	6.2×10^{-6}
3	1	168.31	1.5×10^{-4}	194.12	1.7×10^{-4}	220.31	1.9×10^{-4}	240.37	2.2×10^{-4}
	2	167.35	1.6×10^{-4}	197.98	1.8×10^{-4}	217.62	2.1×10^{-4}	242.06	2.3×10^{-4}
	3	111.51	7.5×10^{-5}	122.20	7.7×10^{-5}	133.16	7.9×10^{-5}	143.78	7.9×10^{-5}
	4	140.48	9.6×10^{-5}	155.02	1.0×10^{-4}	169.66	1.1×10^{-4}	188.09	1.3×10^{-4}
	5	64.31	6.6×10^{-5}	64.62	6.7×10^{-5}	65.04	6.7×10^{-5}	73.58	7.6×10^{-5}
4	1	175.05	1.6×10^{-4}	200.08	1.8×10^{-4}	232.0	2.1×10^{-4}	261.30	2.4×10^{-4}
	2	183.92	1.7×10^{-4}	207.45	1.9×10^{-4}	227.90	2.1×10^{-4}	257.90	2.4×10^{-4}
	3	166.63	7.7×10^{-5}	181.88	7.8×10^{-5}	191.72	8.0×10^{-5}	193.92	8.1×10^{-5}
	4	162.82	9.7×10^{-5}	179.45	1.1×10^{-4}	198.10	1.2×10^{-4}	220.30	1.3×10^{-4}
	5	75.09	7.6×10^{-5}	77.31	7.8×10^{-5}	80.74	8.2×10^{-5}	91.17	9.2×10^{-5}
5	1	192.38	1.9×10^{-4}	217.30	2.2×10^{-4}	237.47	2.5×10^{-4}	268.85	3.2×10^{-4}
	2	194.21	1.8×10^{-4}	231.68	1.9×10^{-4}	271.38	2.2×10^{-4}	295.1	2.5×10^{-4}
	3	218.22	7.8×10^{-5}	240.46	7.9×10^{-5}	256.06	8.1×10^{-5}	256.37	8.2×10^{-5}
	4	181.65	1.0×10^{-4}	197.72	1.2×10^{-4}	216.90	1.3×10^{-4}	237.74	1.4×10^{-4}
	5	85.17	8.5×10^{-5}	87.27	8.7×10^{-5}	89.21	8.9×10^{-5}	93.65	9.5×10^{-5}
6	1	218.84	2.4×10^{-4}	228.49	2.4×10^{-4}	254.99	2.9×10^{-4}	269.46	3.1×10^{-4}
	2	231.42	1.8×10^{-4}	282.21	2.1×10^{-4}	294.68	2.2×10^{-4}	347.95	2.5×10^{-4}
	3	265.29	8.3×10^{-5}	287.74	9.1×10^{-5}	307.20	9.3×10^{-5}	313.61	9.4×10^{-5}
	4	202.50	1.2×10^{-4}	218.28	1.2×10^{-4}	236.07	1.4×10^{-4}	255.18	1.4×10^{-4}
	5	91.96	8.9×10^{-5}	94.02	9.1×10^{-5}	97.01	9.4×10^{-5}	104.0	1.0×10^{-4}

decreases from 2.1×10^{-4} mm/mm to 9×10^{-5} mm/mm for same temperature and deflection case. With increasing temperature, the stress generally increases across all deflection levels with stress values increased from 200.35 MPa to 220.19 MPa when temperature increased from 26 °C to 56 °C in the case of 6 mm deflection. All in all, the highest bracket stress during both the loading and unloading cycles was recorded at 6 mm deflection and 56 °C, with stress magnitudes of 411.02 MPa and 220.19 MPa, respectively. Across all settings, stress values were consistently higher during the loading cycle compared to unloading cycle.

This study examines the mechanical deformation behavior of ceramic bracket slots under varying NiTi archwire deflections and bending temperatures through three-dimensional numerical modeling. The results provide insights into the effect of mechanical loading and thermal fluctuations on bracket performance.

Effect of Wire Deflection and Temperature on Bending Force

NiTi wires, due to their superelasticity, generate controlled bending forces that facilitate bracket displacement and tooth movement. However, improper regulation of these forces may cause bracket deformation, potentially extending the duration of orthodontic treatment. Therefore, a precise understanding of NiTi archwire forces is crucial for ensuring effective and safe orthodontic outcomes. Based on Fig. 5a and Table 2, the deformation of the ceramic bracket exhibited a direct correlation with the loading force exerted by the NiTi wire across varying magnitudes of deflection and bending temperatures. It is evident that higher magnitudes of deflection and elevated bending temperatures resulted in increased loading forces generated by the NiTi wire. Although NiTi wires are recognized for generating constant forces under tensile loading conditions,

Table 3. Stress and strain in ceramic bracket at different deflections and temperatures during unloading.

Deflection case (mm)	Point n o.	26 °C		36 °C		46 °C		56 °C	
		Stress (MPa)	Strain (mm/mm)						
1	1	27.38	1.9×10^{-5}	29.42	2.1×10^{-5}	33.57	2.3×10^{-5}	36.16	2.4×10^{-5}
	2	24.74	2.3×10^{-5}	28.16	2.5×10^{-5}	29.74	2.5×10^{-5}	30.91	2.6×10^{-5}
	3	29.59	3.1×10^{-5}	34.90	3.4×10^{-5}	35.68	3.7×10^{-5}	36.20	3.8×10^{-5}
	4	22.86	3.2×10^{-5}	25.76	3.6×10^{-5}	29.07	4.2×10^{-5}	29.75	4.9×10^{-5}
	5	0.09	8.1×10^{-8}	0.10	9.4×10^{-8}	0.11	1.0×10^{-7}	0.11	1.1×10^{-7}
2	1	46.97	2.5×10^{-5}	58.54	3.3×10^{-5}	67.67	4.8×10^{-5}	81.17	5.5×10^{-5}
	2	39.19	3.4×10^{-5}	50.05	3.5×10^{-5}	58.13	5.7×10^{-5}	69.88	5.6×10^{-5}
	3	39.63	3.3×10^{-5}	46.29	4.6×10^{-5}	56.61	5.3×10^{-5}	63.85	5.8×10^{-5}
	4	28.70	3.7×10^{-5}	35.09	4.5×10^{-5}	54.51	6.6×10^{-5}	68.18	8.2×10^{-5}
	5	0.12	1.1×10^{-7}	0.15	1.4×10^{-5}	0.19	1.7×10^{-5}	0.23	2.1×10^{-5}
3	1	56.91	4.2×10^{-5}	65.38	3.9×10^{-5}	72.10	4.9×10^{-5}	81.69	4.2×10^{-5}
	2	66.2	6.2×10^{-5}	69.98	5.7×10^{-5}	73.77	6.4×10^{-5}	78.74	7.1×10^{-5}
	3	40.2	3.4×10^{-5}	49.12	4.8×10^{-5}	57.48	5.4×10^{-5}	69.33	6.2×10^{-5}
	4	31.39	3.8×10^{-5}	36.83	4.6×10^{-5}	59.07	4.8×10^{-5}	68.80	8.6×10^{-5}
	5	11.80	1.3×10^{-5}	15.33	1.7×10^{-5}	23.14	2.4×10^{-5}	35.20	3.6×10^{-5}
4	1	84.09	6.3×10^{-5}	93.42	6.3×10^{-5}	100.35	6.5×10^{-5}	101.43	6.5×10^{-5}
	2	84.10	7.3×10^{-5}	93.38	7.1×10^{-5}	97.13	6.9×10^{-5}	108.05	7.6×10^{-5}
	3	41.68	1.6×10^{-4}	52.28	5.1×10^{-5}	59.23	6.5×10^{-5}	70.49	6.5×10^{-5}
	4	33.62	6.7×10^{-5}	37.13	5.4×10^{-5}	59.16	5.7×10^{-5}	69.18	9.1×10^{-5}
	5	16.83	4.4×10^{-5}	19.32	5.3×10^{-5}	24.79	6.4×10^{-5}	36.47	7.8×10^{-5}
5	1	87.78	7.4×10^{-5}	106.28	8.4×10^{-5}	116.91	9.1×10^{-5}	122.96	9.1×10^{-5}
	2	123.77	7.3×10^{-5}	146.74	7.9×10^{-5}	149.76	7.9×10^{-5}	162.27	8.1×10^{-5}
	3	42.51	2.9×10^{-4}	54.88	8.6×10^{-5}	60.17	7.1×10^{-5}	74.99	7.2×10^{-5}
	4	35.90	6.8×10^{-5}	39.70	5.6×10^{-5}	60.22	6.3×10^{-5}	75.69	9.3×10^{-5}
	5	17.32	6.9×10^{-5}	79.99	7.9×10^{-5}	91.29	8.9×10^{-5}	105.60	1.0×10^{-4}
6	1	88.72	7.7×10^{-5}	107.01	9.1×10^{-5}	117.05	9.2×10^{-5}	124.91	9.3×10^{-5}
	2	135.59	7.3×10^{-5}	147.85	8.2×10^{-5}	158.67	8.4×10^{-5}	175.39	8.5×10^{-5}
	3	59.43	3.6×10^{-4}	67.56	9.5×10^{-5}	78.97	9.1×10^{-5}	95.20	9.3×10^{-5}
	4	40.68	7.1×10^{-5}	46.58	6.3×10^{-5}	62.11	6.7×10^{-5}	78.43	9.9×10^{-5}
	5	94.41	9.3×10^{-5}	99.37	9.5×10^{-5}	105.89	1.0×10^{-4}	116.55	1.1×10^{-4}



such consistent force behavior is seldom observed when the wire is deformed in a three-bracket configuration. The progressive increase in loading force magnitude at higher deflections as seen in Fig. 5a can be attributed to the rising frictional forces experienced by the wire as it slides along the bracket corners with sharper wire curvatures at high deflection case. As the wire encounters greater friction during sliding, it exerts increased pressure on the ceramic bracket corners, resulting in more significant bracket deformation. This direct relationship between sliding friction and wire curvature is supported by the findings of Lee and Hwang, who demonstrated that higher sliding friction occurs when the wire is guided through brackets with greater angulation [23].

Additionally, the gradual increase in the loading force of the NiTi wire with rising bending temperature is primarily due to its temperature-dependent phase transformation behavior, which follows the Clausius-Clapeyron relationship. As the temperature increases, a higher stress is required to induce the martensitic-to-austenitic cycle transformation in NiTi wires. This phenomenon corresponds to the stress-temperature rate of 6.7 MPa/°C, as specified in Table 1, which was determined from the variation in the loading and unloading plateaus of the NiTi wire under tension at different temperatures. At higher temperatures, the austenitic cycle becomes more thermodynamically stable, increasing the wire's stiffness and resistance to deformation. Consequently, a greater force is needed to initiate the stress-induced martensitic transformation

at elevated temperatures compared to lower temperatures. Similar findings were reported by Mona et al [24], who observed a rise in force levels with increasing temperature and wire deflection.

It is interesting to note that the unloading force as shown in Fig. 5b was positive for deflections of 1 mm to 4 mm but became negative for deflection cases of 5 and 6 mm. The negative force arises due to the increased bending curvature of the wire around the bracket corners at high deflections. This causes the wire to press more firmly against the bracket surface, restricting its sliding movement within the three-bracket arrangement. In this constrained state, the reference point of the middle bracket RP-1 is unable to accurately capture the springback force from the wire during the unloading cycle, resulting in a negative force measurement as the unloading cycle progresses. Despite the negative force values, the mechanical interlocking between the wire and the bracket slot induces significant deformation of the bracket itself, with stress magnitudes ranging from 40.68 to 175.39 MPa in the case of 6 mm deflection. In contrast, this negative force behavior is not observed at lower deflections (4 mm or less). At these smaller deflections, the wire curvature remains less pronounced, allowing the NiTi wire to slide more freely within the bracket slots. As a result, the stress magnitude recorded on the bracket model is significantly lower at all interested points, ranging from 0.09 to 36.20 MPa in the case of 1 mm deflection, as shown in Table 3. The dependence of archwire force on applied deflection has been reported by Gatto et

Table 4. Maximum stress and strain in ceramic bracket slot during loading and unloading.

Deflection case (mm)	26 °C		36 °C		46 °C		56 °C		
	Stress (MPa)	Strain (mm/mm)	Stress (MPa)	Strain (mm/mm)	Stress (MPa)	Strain (mm/mm)	Stress (MPa)	Strain (mm/mm)	
Loading	1	172.9	2.7×10^{-4}	189.6	2.9×10^{-4}	196.3	3.1×10^{-4}	201.91	3.2×10^{-4}
	2	226.6	3.4×10^{-4}	245.5	3.6×10^{-4}	280.2	4.1×10^{-4}	317.43	4.6×10^{-4}
	3	249.3	3.7×10^{-4}	286.9	4.2×10^{-4}	329.2	4.7×10^{-4}	338.43	5.2×10^{-4}
	4	266.4	4.2×10^{-4}	321.3	4.6×10^{-4}	337.3	5.1×10^{-4}	376.40	7.7×10^{-4}
	5	280.2	4.3×10^{-4}	321.6	4.8×10^{-4}	366.5	5.4×10^{-4}	403.23	8.8×10^{-4}
	6	327.8	4.8×10^{-4}	336.7	5.3×10^{-4}	384.8	7.9×10^{-4}	411.02	9.2×10^{-4}
Unloading	1	41.80	9.4×10^{-5}	44.76	1.1×10^{-4}	50.35	1.2×10^{-4}	51.49	1.2×10^{-4}
	2	75.80	1.5×10^{-4}	98.08	1.9×10^{-4}	135.75	2.1×10^{-4}	143.33	2.3×10^{-4}
	3	163.94	1.7×10^{-4}	172.33	2.0×10^{-4}	184.77	2.2×10^{-4}	197.48	2.3×10^{-4}
	4	170.34	2.0×10^{-4}	182.28	2.1×10^{-4}	195.56	2.3×10^{-4}	199.34	2.5×10^{-4}
	5	173.63	2.1×10^{-4}	187.71	2.2×10^{-4}	208.47	2.4×10^{-4}	208.31	2.6×10^{-4}
	6	200.35	2.1×10^{-4}	203.43	2.9×10^{-4}	209.19	2.9×10^{-4}	220.19	2.9×10^{-4}

al. [25], who found that wires subjected to greater deflections release lower deactivation forces during unloading.

Bracket Failure Risks and Clinical Implications

Based on Table 4, it is confirmed that the ceramic bracket can experience stress up to 411.02 MPa during loading and 220.19 MPa during unloading within the bending conditions considered in this study. Assuming a fracture strength of approximately 117.76 MPa for the ceramic bracket [16], the maximum stresses experienced by the ceramic bracket during loading at all temperatures and deflection cases exceeded this value. Specifically, at higher deflection cases of 5 mm and 6 mm, the stress values significantly surpass this threshold, particularly at 46 °C and 56 °C, where the maximum recorded stresses reach 384.8 MPa and 411.02 MPa, respectively. These findings suggest a high likelihood of fracture under clinical conditions involving substantial wire activation and elevated oral temperatures. Despite the high bracket stress magnitude, this study primarily focuses on the stresses recorded during the unloading cycle, as they relate to the continuous pressure exerted on the ceramic bracket throughout the orthodontic treatment period. It is noteworthy that among the deflections and temperatures examined in this study, the ceramic bracket is expected to withstand failure only under bending conditions up to a 2 mm deflection at 36 °C. At this point, the recorded bracket stress was 98.08 MPa. However, increasing the NiTi wire deflection and temperature beyond this threshold can elevate stress levels to as much as 220 MPa, thereby increasing the risk of bracket failure.

Based on the observed direct relationship between wire deflection, bending temperature, and bracket stress levels in this study, it is advisable for patients with severe malocclusion to avoid consuming hot foods and beverages. The rationale behind this recommendation is that elevated temperatures can increase the stiffness of NiTi archwires, resulting in higher forces exerted on the ceramic brackets, and hence stress the bracket beyond its fracture strength. Additionally, a higher loading force may exacerbate patient discomfort during archwire insertion [26]. For cases involving large deflections, it is advisable to use smaller, lighter, or round NiTi archwires rather than rectangular ones. Round archwires are

less stiff, thereby reducing the amount of stress applied to the brackets, which can help mitigate the risk of bracket failure. Using rectangular NiTi archwires, particularly at high temperatures and large deflections, increases the likelihood of excessive stress accumulation within the ceramic brackets, which may exceed their fracture strength. Additionally, to further enhance bracket durability and accommodate different stages of orthodontic treatment, future bracket designs could incorporate adjustable slot room sizes. By allowing more room for play, the bracket slot could adapt to the archwire's size and deflection, thereby minimizing excessive stress buildup. This adjustable feature would enable better force distribution and reduce the risk of bracket failure, particularly during early treatment stages when larger deflections are common.

CONCLUSION

This study investigates the mechanical deformation behavior of ceramic bracket slots under varying wire deflections and temperatures. The finite element analysis demonstrated that the bracket deformation was consistently concentrated at the corner areas of the slots across all three ceramic brackets model. Increasing the bending deflection and temperature significantly elevate stress levels within the ceramic brackets, often exceeding their fracture strength, particularly during the loading cycle. The maximum stress recorded during the loading cycle was 411.02 MPa at 56 °C for a 6 mm deflection. Although the unloading cycle was less severe, it still posed failure risks for deflections beyond 2 mm. In this cycle, the maximum recorded stress was 220.19 MPa at 56 °C for a 6 mm deflection.

ACKNOWLEDGMENTS

The authors are grateful for the financial support provided by Universiti Sains Malaysia for Graduate on Time incentive with account number: R502-KR-GOT001-0000001255-K134.

CONFLICT OF INTEREST

The authors declare that there is no conflict of interests regarding the publication of this manuscript.

REFERENCES

1. Razali MF, Mahmud AS, Mokhtar N. Force delivery of NiTi orthodontic arch wire at different magnitude of deflections

- and temperatures: A finite element study. *J Mech Behav Biomed Mater.* 2018;77:234-241.
2. Harikrishnan P, Magesh V, Ajayan AM, JebaSingh DK. Finite element analysis of torque induced orthodontic bracket slot deformation in various bracket-archwire contact assembly. *Computer Methods and Programs in Biomedicine.* 2020;197:105748.
 3. Lee YY, Izham N, Mohd Zulkifly MF, Mohamed Mustafar MF, Ismail AK, Mohamed Shah NFFN, et al. The Brain-Gut Clinic in Hospital Universiti Sains Malaysia: Pioneering New Service to Advance Neuro-Gastroenterology and Motility in Malaysia. *The Malaysian journal of medical sciences : MJMS.* 2023;30(3):1-7.
 4. Magesh V, Harikrishnan P, Chandra Sekhar T. Finite element analysis of orthodontic bracket tie wing deformation due to labial crown torque. *IOP Conference Series: Materials Science and Engineering.* 2018;402:012085.
 5. Moresca R. Orthodontic treatment time: can it be shortened? *Dental Press J Orthod.* 2018;23(6):90-105.
 6. Abbing A, Koretsi V, Eliades T, Papageorgiou SN. Duration of orthodontic treatment with fixed appliances in adolescents and adults: a systematic review with meta-analysis. *Prog Orthod.* 2020;21(1):37-37.
 7. Papageorgiou SN, Höchli D, Eliades T. Outcomes of comprehensive fixed appliance orthodontic treatment: A systematic review with meta-analysis and methodological overview. *Korean journal of orthodontics.* 2017;47(6):401-413.
 8. Sarver D, William R. Proffit, 1936-2018. *Am J Orthod Dentofacial Orthop.* 2019;155(1):146-147.
 9. Khamashta-Ledezma L. *Archwires. Preadjusted Edgewise Fixed Orthodontic Appliances: Wiley;* 2021. p. 175-201.
 10. Prakash S, Armijo AD, Masel RI, Shannon MA. Unsteady Flames in Microcombustion. *Energy Conversion and Resources;* 2006/01/01: ASMEDC; 2006. p. 363-364.
 11. Alcaraz I, Moyano J, Pàmies A, Ruiz G, Artés M, Gil J, et al. Properties of Superelastic Nickel-Titanium Wires after Clinical Use. *Materials (Basel, Switzerland).* 2023;16(16):5604.
 12. Papageorgiou SN, Keilig L, Hasan I, Jäger A, Bourauel C. Effect of material variation on the biomechanical behaviour of orthodontic fixed appliances: a finite element analysis. *Eur J Orthod.* 2016;38(3):300-307.
 13. Polychronis G, Papageorgiou SN, Riollo CS, Panayi N, Zinelis S, Eliades T. Fracture toughness and hardness of in-office, 3D-printed ceramic brackets. *Orthodontics & Craniofacial Research.* 2023;26(3):476-480.
 14. AlBadr AH, Talic NF. Testing the tensile fracture strength tie-wings of different orthodontic ceramic bracket using an Instron machine. *The Saudi dental journal.* 2023;35(8):1048-1052.
 15. Kim KN, Lee SB, Kim HJ, Choi JS, Kim KM, Hwang CJ. Fracture Strength of Ceramic Bracket Tie Wings Subjected to Force Direction. *Key Engineering Materials: Trans Tech Publications Ltd.;* 2007. p. 1353-1356.
 16. Sanchez DJ, Walker MP, Kula K, Williams KB, Eick JD. Fluoride Prophylactic Agents Effect on Ceramic Bracket Tie-Wing Fracture Strength. *The Angle Orthodontist.* 2008;78(3):524-530.
 17. Ghosh J, Nanda RS, Duncanson MG, Currier GF. Ceramic bracket design: An analysis using the finite element method. *Am J Orthod Dentofacial Orthop.* 1995;108(6):575-582.
 18. Akin PC, Nanda RS, Duncanson MG, Currier GF, Sinha PK. Fracture strength of ceramic brackets during arch wire torsion. *Am J Orthod Dentofacial Orthop.* 1996;109(1):22-27.
 19. Magesh V, Harikrishnan P. Stress distribution in ceramic orthodontic bracket, tooth, bone and PDL contact assembly - A finite element study. *IOP Conference Series: Materials Science and Engineering.* 2020;912(2):022019.
 20. Nucera R, Gatto E, Borsellino C, Aceto P, Fabiano F, Matarese G, et al. Influence of bracket-slot design on the forces released by superelastic nickel-titanium alignment wires in different deflection configurations. *The Angle orthodontist.* 2014;84(3):541-547.
 21. Shah UH, Singla A, Mahajan V, Jaj HS, Dhiman I, Thakur S. Comparison of Slot Deformation in Different Types of Bracket During Torque Application—A Finite Element Study. *Journal of Indian Orthodontic Society.* 2023.
 22. Abraham J, Diller K. A Review of Hot Beverage Temperatures—Satisfying Consumer Preference and Safety. *J Food Sci.* 2019;84(8):2011-2014.
 23. Lee SM, Hwang C-J. A comparative study of frictional force in self-ligating brackets according to the bracket-archwire angulation, bracket material, and wire type. *Korean journal of orthodontics.* 2015;45(1):13-19.
 24. Ahmed MN, Motawea IT, Ibrahim SA, Elkady RM. Influence of Intra-Oral Temperature Changes on The Mechanical Properties of Different Nickel Titanium Orthodontic Arch-Wires. *Al-Azhar Journal of Dentistry.* 2024;11(2).
 25. Gatto E, Matarese G, Di Bella G, Nucera R, Borsellino C, Cordasco G. Load-deflection characteristics of superelastic and thermal nickel-titanium wires. *The European Journal of Orthodontics.* 2011;35(1):115-123.
 26. Hsu H-M, Chen K-C, Chang C-J, Lee T-M, Liu J-K. Load-Deflection Behaviors of Superelastic NiTi Wires Using Two Bending Test Methods Including Passive Self-Ligating Brackets. *Taiwanese Journal of Orthodontics.* 2024;36(1).